

---

# Give Me Your Trained Model: Domain Adaptive Semantic Segmentation without Source Data

---

Yuxi Wang<sup>1,2</sup> Jian Liang<sup>2</sup> Zhaoxiang Zhang<sup>1,2,3</sup> \*

<sup>1</sup> University of Chinese Academy of Sciences

<sup>2</sup> Center for Research on Intelligent Perception and Computing, CASIA

<sup>3</sup> Center for Excellence in Brain Science and Intelligence Technology, CAS

liangjian92@gmail.com

{wangyuxi2016, zhaoxiang.zhang}@ia.ac.cn

## Abstract

Benefited from considerable pixel-level annotations collected from a specific situation (source), the trained semantic segmentation model performs quite well, but fails in a new situation (target) due to the large domain shift. To mitigate the domain gap, previous cross-domain semantic segmentation methods always assume the co-existence of source data and target data during distribution alignment. However, the access to source data in the real scenario may raise privacy concerns and violate intellectual property. To tackle this problem, we focus on an interesting and challenging cross-domain semantic segmentation task where only the trained source model is provided to the target domain, and further propose a unified framework called Domain Adaptive Semantic Segmentation without Source data (DAS<sup>3</sup> for short). Specifically, DAS<sup>3</sup> consists of three schemes, *i.e.*, feature alignment, self-training, and information propagation. First, we mainly develop a focal entropic loss on the network outputs to implicitly align the target features with unseen source features via the provided source model. Second, besides positive pseudo labels in vanilla self-training, we first introduce negative pseudo labels to the field and develop a bi-directional self-training strategy to enhance the representation learning in the target domain. Finally, the information propagation scheme further reduces the intra-domain discrepancy within the target domain via pseudo semi-supervised learning. Extensive results on synthesis-to-real and cross-city driving datasets validate DAS<sup>3</sup> yields state-of-the-art performance, even on par with methods that need access to source data.

## 1 Introduction

Semantic segmentation is a fundamental task in the computer vision field that aims to estimate the pixel-level predictions for a given image. Despite the rapid progress on deep learning-based methods, attaining high performance usually demands vast amounts of training data with pixel-level annotations. However, collecting large-scale datasets tends to be prohibitively expensive and time-consuming. Alternatively, previous cross-domain learning approaches [1–5] attempt to train a satisfactory segmentation model for unlabeled real-world data (called target domain) by exploiting labeled photo-realistic synthetic images (*e.g.*, GTA5 [6] and SYNTHIA [7]) or other existing real-world datasets (called source domain). However, due to the domain discrepancy, a well-performing model trained on the source domain degrades drastically when applied to the target domain. To remedy this issue, various domain alignment strategies are proposed in [8, 2, 9–11].

---

\*Corresponding author

The essential idea for domain adaptive semantic segmentation is to effectively transfer the knowledge learned from a distinct source domain to a target domain. Previous methods achieve this goal by bridging the domain gap in the image level [12, 13, 10, 14, 15, 5, 16], feature level [17, 8, 9], and output level [2–4, 18]. Although these approaches have made remarkable progress, they usually require access to the labeled source data during the alignment process. However, in some crucial scenarios, the source data is inaccessible due to data protection laws. Thus, this paper addresses a challenging source data-free domain adaptation setting for semantic segmentation, where only the trained source model instead of the source data is provided to the target domain for adaptation.

Due to the absence of source data, previous domain alignment methods are not feasible anymore under the source data-free setting. Recent studies employ model adaptation [19] or generated synthetic fake source data [20] to tackle the source-data absent problem. Although they obtain promising results, it highly relies on the prior knowledge of the source model and partially ignores the target-specific information, leading to sub-optimal solutions. In this paper, we propose a new framework called Domain Adaptive Semantic Segmentation without Source data (DAS<sup>3</sup>), which focuses on fully exploiting the target knowledge to adapt by implicitly minimizing the domain discrepancy and explicitly learning self-supervised feature representations. DAS<sup>3</sup> mainly consists of three schemes, *i.e.*, feature alignment, self-training, and information propagation. First, the implicit feature alignment scheme assumes the source domain and the target domain share the same classifier layer and enforces the target feature representations fitting to the source classifier. To achieve this, we develop a focal entropic loss on the network outputs to implicitly align target features with unseen source features via the provided source model. Second, during the bi-directional self-training process, we first introduce negative pseudo-labeling to the domain adaptation field. Specifically, the negative pseudo labels refer to the predictions with low confidence scores, providing solid supervised information to indicate the absent classes for the corresponding pixels. We further consider vanilla positive pseudo labels with high confidence scores and develop a bi-directional self-training strategy to enhance the target representation learning. Finally, the information propagation scheme aims to reduce the intra-domain discrepancy within the target domain. Particularly, we divide the target domain into two parts and employ a semi-supervised learning technique, ClassMix [21], to boost the adaptation performance, which acts as a generic simple and effective post-processing module for domain adaptation.

The main contributions of this paper can be summarized as follows. 1) We propose a novel source data-free domain adaptation method for semantic segmentation that only requires the source model and unlabeled target data without access to the source data. 2) We develop a new focal entropic objective loss for implicitly aligning the features of source and target domains. 3) We propose a new bi-directional self-training strategy that considers both the positive pseudo labels and negative pseudo labels. 4) The proposed method yields state-of-the-art cross-domain results with the Cityscapes [22] segmentation mIoU by 50.7 and 52.1 when adapting from GTA5 [6] and SYNTHIA [7]. Moreover, it performs on par with domain adaptation methods with accessing the source data.

## 2 Related Work

**Domain Adaptive Semantic Segmentation.** Existing domain adaptation methods for semantic segmentation can be roughly categorized into two groups: adversarial learning based methods and self-supervised learning based methods. For adversarial learning, numerous works focus on reducing the distribution misalignment in the image level [12, 13, 10, 14, 15, 5, 16], feature level [17, 8, 9], and output level [2–4, 18]. For the self-supervised learning method, the essential idea is to generate reliable pseudo labels. Typical approaches usually consist of two steps: 1) generate pseudo labels based on the source model [23, 24] or the learnt domain-invariant model [25–27], 2) refine the target model supervised by the generated pseudo labels. Although these methods have achieved promising results, they usually heavily depend on the labeled source data during adaptation. In this paper, we address a challenging source data-free domain adaptation setting without any raw source data due to the data privacy policy.

**Source Data-free Domain Adaptation.** To tackle source data-free domain adaptation problem, a few recent methods [28–30] provide kinds of model adaptation solutions for classification problems. [31] proposes a universal source data-free domain adaptation when the knowledge of the label space in the target domain is not available. As for semantic segmentation tasks, model adaptation is also a feasible method to tackle the source data absent setting. Specifically, [20] leverages a generative model to synthesize fake samples for estimating the source distribution, and preserve source domain

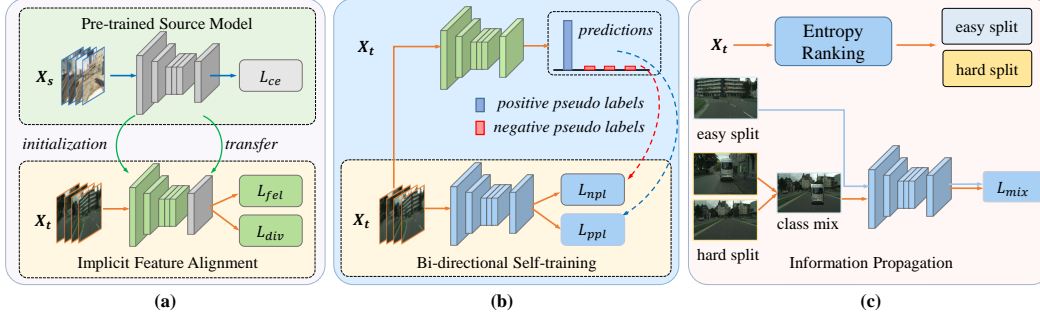


Figure 1: Illustration of the proposed Domain Adaptive Semantic Segmentation without Source data (DAS<sup>3</sup>) framework. (a) is the implicit feature alignment. We freeze the classifier and train the feature extractor to achieve implicit feature alignment by minimizing  $\mathcal{L}_{fel}$  and  $\mathcal{L}_{div}$ . (b) illustrates the process of bi-directional self-training. Positive and negative pseudo labels are obtained from a fixed model initialized from stage (a). (c) illustrates the process of information propagation. The target data is divided into easy and hard splits according to the entropy ranking, and then we reduce intra-domain discrepancy in a semi-supervised manner by minimizing loss  $\mathcal{L}_{mix}$ .

knowledge via knowledge transfer during model adaptation. [19] proposes an uncertainty-reducing method to enhance feature representation. In contrast, we propose a simple and effective framework for semantic segmentation tasks, which exploits the target-specific knowledge to intensify the target feature learning.

**Semi-supervised Learning.** The key for semi-supervised learning is to learn a consistent representation between the labeled and unlabeled data. To achieve this goal, consistency regularization methods have been heavily studied in recent years. [32] first introduces perturbations into the input that changes output predictions mostly. Then the augmentation is adopted as solid perturbations. [33] uses the Mixup as the consistency regularization. [34] uses auto-augmentation to generate augmented inputs, and [35] extends the idea by dividing the augmentation set into strong and weak operations. In this work, we refer the semi-supervised learning strategy to domain adaptation, aiming to reduce the intra-domain discrepancy within the target domain.

### 3 Method

We aim to address source-data absent domain adaptive semantic segmentation problem with only a pre-trained source model in this paper. Specifically, we are given  $n_s$  labeled images  $\{x_s^i, y_s^i\}_{i=1}^{n_s}$  from the source domain  $\mathcal{D}_s$  and  $n_t$  unlabeled images  $\{x_t^i\}_{i=1}^{n_t}$  from the target domain  $\mathcal{D}_t$ , where  $x_s^i \in \mathcal{X}_s$ ,  $y_s^i \in \mathcal{Y}_s$ , and  $x_t \in \mathcal{X}_t$ . Our goal is to learn a segmentation mapping  $\mathcal{M}_t : \mathcal{X}_t \rightarrow \mathcal{Y}_t$  transferring from the source mapping  $\mathcal{M}_s : \mathcal{X}_s \rightarrow \mathcal{Y}_s$ , which predicts a pixel-wise label  $y_t^i \in \mathcal{Y}_t$  for a given image  $x_t^i$ . In this work, we only access target images  $\{x_t^i\}_{i=1}^{n_t}$  and the trained source mapping  $\mathcal{M}_s$ .

The semantic segmentation model  $\mathcal{M}_s$  on the source domain is obtained in a supervised manner by minimizing the following cross-entropy loss,

$$\mathcal{L}_{ce} = -\frac{1}{n_s} \sum_{i=1}^{n_s} \sum_{j=1}^{H \times W} \sum_{c=1}^C y_s^{(i,j,c)} \log p_s^{(i,j,c)}, \quad (1)$$

where  $n_s$  is the number of source images,  $H$  and  $W$  denote the image size, and  $C$  is the number of categories.  $p_s^{(i,j,c)}$  denotes the predicted category probability by  $\mathcal{M}_s$  and the  $y_s^{(i,j,c)}$  is the corresponding one-hot ground-truth label. Generally, the segmentation model  $\mathcal{M}_s$  consists of a feature extractor  $f_s$  and a classifier  $g_s$ , i.e.,  $\mathcal{M}_s = f_s \circ g_s$ .

To transfer the trained  $\mathcal{M}_s$  to the target domain, our proposed DAS<sup>3</sup> framework mainly includes three stages, shown in Figure 1. Stage (a) is the implicit feature alignment, which implicitly enforces the target feature to fit the source model via the proposed focal entropic loss and weighted diversity loss, referring to Section 3.1. In this stage, the target model is initialized by  $\mathcal{M}_s$  and the classifier is frozen during training. Stage (b) is the self-training process, which enhances target feature representation

learning by the proposed bi-directional self-training technique described in Section 3.2. Finally, in stage (c), we achieve information propagation in a semi-supervised manner, which reduces the intra-domain discrepancy and boosts the adaptation performance with a significant improvement. We will elaborate on the details in the following.

### 3.1 Implicit Feature Alignment

We incorporate the entropy minimization strategy to eliminate the distribution gap in this section. Although several previous methods [4, 36] have made progress, the different transferable degrees of target pixels are ignored. For example, predictions with high confidence values should have a higher transferability than those with low confidence scores, and vice versa. Unlike existing methods treating all pixels equally, we exploit a focal entropic loss that expects to down-weight the contribution of uncertain predictions and rapidly focus the model on certain predictions. Inspired by [37], we propose a focal entropic loss as follows:

$$\mathcal{L}_{fel} = \alpha * (1 - h(x_t))^\gamma * h(x_t), \quad (2)$$

where  $\alpha$  balances the importance of certain/uncertainty predictions and  $\gamma$  controls the weight of certain samples that own smaller entropy values.  $h(x_t) = -\sum_{c=1}^C p_{x_t}^{(h,w,c)} \log p_{x_t}^{(h,w,c)}$  denotes the entropy map for a given target image  $x_t$ .  $p_{x_t}^{(h,w,c)}$  is the predicted probability of the target image  $x_t$ , i.e.,  $p_{x_t}^{(h,w,c)} = f_t \circ g_t(x_t)$ .  $f_t$  and  $g_t$  denote the feature extractor and classifier for the target data, which are initialized by the trained source model  $f_s$  and  $g_s$ , respectively. Notice that we fix the classifier  $g_t$  in this process by the assumption of the source and target module using the same classifier. Furthermore, to ensure the global diversity of the target outputs, we adopt a diversity-promoting loss specified in [28] and propose a confidence-weighted diversity objective as below,

$$\mathcal{L}_{div} = \sum_{c=1}^C \hat{p}_{x_t}^{(h,w,c)} \log \hat{p}_{x_t}^{(h,w,c)}, \quad (3)$$

where  $\hat{p}_{x_t}^{(h,w,c)}$  is the weighted mean output embedding of the target image  $x_t$ . The weight is calculated based on the entropy  $h(x_t)$  and  $\hat{p}_{x_t}^{(h,w,c)} = \sum_{(h,w)} \exp(-\lambda * h(x_t)) * p_{x_t}^{(h,w,c)}$ .  $\lambda$  is a hyper-parameter and we empirically set  $\lambda = 3$  in all experiments. This technique can circumvent the problem of wrongly predicting confusing target instances as relatively easy classes to learn.

### 3.2 Bi-directional Self-training

Previous self-supervised learning methods focus on strengthening the reliability of pseudo labels by developing various denoising strategies, but they ignore most of the pixels with lower prediction confidence scores. In that case, the model tends to be over-fitting because the selected over-confident samples lack references using negative pseudo labels. To remedy this, we restrict our attention to the predictions with lower confidence values, termed negative pseudo labels. Although low-confidence predictions cannot be assigned as the correct labels, they will definitely indicate specific absent classes. As Figure 2 shows, it is hard to clearly indicate which category it belongs to for the ignore pixels (black areas), but it is easy to determine which categories it does not belong to. Inspired by this, we propose a bi-directional self-training method that includes positive pseudo labeling and negative pseudo labeling.

**Positive pseudo labeling.** We first introduce the positive pseudo labeling method, which aims to select correct pseudo labels with high confidence scores for training. Considering the domain-transfer difficulty among categories, generating pseudo labels according to high confidence will cause hard-to-transfer categories to be ignored. Because easy-to-transfer classes (e.g., roads, buildings, walls, sky)

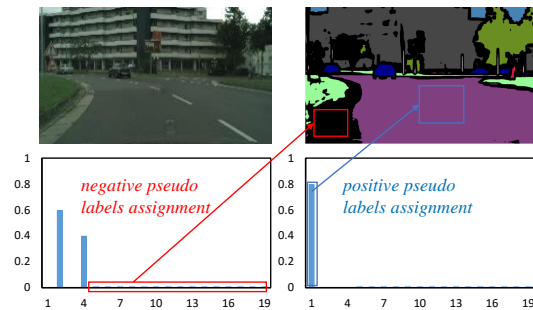


Figure 2: Bi-directional pseudo labels. Blue refers to positive pseudo labels and red refers to negative pseudo labels.

usually have higher prediction confidence scores, while hard-to-transfer classes (*e.g.*, lights, signals, trains, bicycles) perform poorly. Consequently, we assign pseudo-labels based on the guidance of the category-level threshold inspired by [23] as below,

$$\hat{y}_{x_t}^{(h,w,c)} = \begin{cases} 1 & \text{if } c = \operatorname{argmax}_c p_{x_t}^{(h,w,c)} \cap p_{x_t}^{(h,w,c)} > \lambda_c \\ 0 & \text{otherwise,} \end{cases} \quad (4)$$

where  $\lambda_c$  is a category-level threshold that is determined by the top  $K$  predictions within the class  $c$ . Then, we optimize the target model by minimize the categorical cross-entropy with every pseudo label  $\hat{y}_t$ :

$$\mathcal{L}_{ppl} = -\frac{1}{n_t} \sum_{i=1}^{n_t} \sum_{j=1}^{H \times W} \sum_{c=1}^C \hat{y}_t^{(i,j,c)} \log p_t^{(i,j,c)}, \quad (5)$$

where  $n_t$  is the number of target images,  $p_t^{(i,j,c)}$  denotes the predicted category probability, and  $\hat{y}_t^{(i,j,c)}$  is the corresponding pseudo label obtained from Eq. (4).

**Negative pseudo labeling.** For the negative pseudo-label assignment, our goal is to explore the implicit knowledge in uncertainty-aware regions that have been ignored in previous works. Although these predictions have higher uncertainty due to the uniform or low prediction scores, they can definitely point out the absent categories. For example, for a pixel whose output is [0.48, 0.47, 0.02, 0.03], it is impossible to determine which category it belongs to, but we can confidently point out that it does not belong to classes with scores of 0.02 and 0.03. Therefore, we use all absent classes as supervision information for target feature learning. Formally, we assign the negative pseudo labels as follows:

$$\delta(p_{x_t}^{(h,w,c)}) = \begin{cases} 1 & \text{if } p_{x_t}^{(h,w,c)} < \lambda_{neg}, \\ 0 & \text{otherwise,} \end{cases} \quad (6)$$

where  $\lambda_{neg}$  is the negative threshold and we use  $\lambda_{neg} = 0.05$  for all experiments. It is worth noticing that the negative pseudo labels are binary multi-labels, which certainly indicates the absence of relative classes. Then the negative pseudo labeling objective is formulated as follows:

$$\mathcal{L}_{npl} = -\frac{1}{n_t} \sum_{i=1}^{n_t} \sum_{j=1}^{H \times W} \sum_{c=1}^C \delta(p_t^{(i,j,c)}) \log(1 - p_t^{(i,j,c)}). \quad (7)$$

Finally, the bi-directional self-training objective includes the positive and negative pseudo labeling:

$$\mathcal{L}_{bst} = \mathcal{L}_{ppl} + \mathcal{L}_{npl}. \quad (8)$$

### 3.3 Information Propagation

Even we propose a much better solution for global adaptation without source data, intra-domain discrepancy still exists as previous works [36, 20] indicate. Inspired by the self-supervised intra-domain alignment method [36], we first divide the target data into easy and hard splits and then close the intra-domain gap to boost the adaptation performance. Contrary to the traditional adversarial mechanism, we borrow a semi-supervised learning scheme by considering the easy split as labeled data and the hard split unlabeled. As such, the target domain is separated using the entropy ranking strategy as below,

$$r(x_t) = \frac{1}{HW} \sum_{h=1}^H \sum_{w=1}^W h(x_t)^{(h,w)}, \quad (9)$$

which is the mean entropy for a target image  $x_t$  with the corresponding entropy map  $h(x_t)$ . Easy and hard splits are conducted from the ranking of  $r(x_t)$  following  $ratio = \frac{\|x_{te}\|}{(\|x_{te}\| + \|x_{th}\|)}$ , where  $x_{te}$  and  $x_{th}$  denote the easy and hard samples, respectively. We set  $ratio = 0.3$  in our experiments. After that, we incorporate the augmentation strategy in the hard split to regularize the semi-supervised learning. Specifically, we employ the ClassMix [21] technique as below,

$$\mathcal{L}_{mix} = \mathcal{L}_{ce}(\mathcal{M}_t(x_{te}), \hat{y}_{te}) + \mathcal{L}_{ce}(\mathcal{M}_t(\mathbf{Mix}(x_{th}^i, x_{th}^j)), \mathcal{M}'_t(\mathbf{Mix}(x_{th}^i, x_{th}^j))), \quad (10)$$

Table 1: Results of GTA5  $\rightarrow$  Cityscapes. ‘‘SF’’ denotes the source data-free setting. **Red** is the best result for source data-free methods and **blue** is the best result for source data-dependent methods.

Method	SF	road	side.	build.	wall	fence	pole	light	sign	vege.	terr.	sky	person	rider	car	truck	bus	train	motor.	bike	mIoU
Source Only	-	75.8	16.8	77.2	12.5	21.0	25.5	30.1	20.1	81.3	24.6	70.3	53.8	26.4	49.9	17.2	25.9	6.5	25.3	36.0	36.5
AdaptSeg [2]	✗	86.5	36.0	79.9	23.4	23.3	23.9	35.2	14.8	83.4	33.3	75.6	58.5	27.6	73.7	32.5	35.4	3.9	30.1	28.1	42.4
ADVENT [4]	✗	89.4	33.1	81.0	26.6	26.8	27.2	33.5	24.7	83.9	36.7	78.8	58.7	30.5	84.8	38.5	44.5	1.7	<b>31.6</b>	32.4	45.5
CBST [23]	✗	91.8	<b>53.5</b>	80.5	32.7	21.0	34.0	28.9	20.4	83.9	34.2	80.9	53.1	24.0	82.7	30.3	35.9	16.0	25.9	42.8	45.9
CAG_UDA [42]	✗	90.4	51.6	83.8	34.2	27.8	<b>38.4</b>	25.3	<b>48.4</b>	85.4	38.2	78.1	58.6	<b>34.6</b>	84.7	21.9	42.7	<b>41.1</b>	29.3	37.2	50.2
PLCA [43]	✗	84.0	30.4	82.4	<b>35.3</b>	24.8	32.2	36.8	24.5	<b>85.5</b>	37.2	78.6	<b>66.9</b>	32.8	<b>85.5</b>	40.4	48.0	8.8	29.8	41.8	47.7
SIM [44]	✗	90.6	44.7	<b>84.8</b>	34.3	<b>28.7</b>	31.6	35.0	37.6	84.7	<b>43.3</b>	<b>85.3</b>	57.0	31.5	83.8	<b>42.6</b>	48.5	1.9	30.4	39.0	49.2
FDA [5]	✗	<b>92.5</b>	53.3	82.4	26.5	27.6	36.4	<b>40.6</b>	38.9	82.3	39.8	78.0	62.6	34.4	84.9	34.1	<b>53.1</b>	16.9	27.7	<b>46.4</b>	<b>50.5</b>
SFDA [20]	✓	84.2	39.2	82.7	27.5	22.1	25.9	31.1	21.9	82.4	30.5	<b>85.3</b>	58.7	22.1	80.0	33.1	31.5	3.6	27.8	30.6	43.2
Sivaparased [19]	✓	<b>92.3</b>	55.2	81.6	30.8	18.8	<b>37.1</b>	17.7	12.1	84.2	35.9	83.8	57.7	24.1	81.7	27.5	44.3	6.9	24.1	40.4	45.1
DAS <sup>3</sup> (a)	✓	84.7	29.3	80.5	28.3	15.8	19.8	28.3	17.5	83.4	34.9	77.3	58.8	21.8	83.3	30.9	36.6	<b>7.1</b>	29.5	29.7	42.1
DAS <sup>3</sup> (b)	✓	84.6	37.8	83.1	29.9	22.1	25.0	30.8	25.4	84.9	43.7	81.0	59.5	23.8	85.5	35.2	50.7	1.3	32.9	49.8	46.7
DAS <sup>3</sup> (c)	✓	92.2	<b>55.9</b>	<b>84.0</b>	<b>38.7</b>	<b>22.9</b>	27.6	<b>33.9</b>	<b>30.7</b>	<b>86.8</b>	<b>47.1</b>	82.0	<b>61.6</b>	<b>24.5</b>	<b>87.2</b>	<b>40.6</b>	<b>51.2</b>	2.1	<b>41.9</b>	<b>55.1</b>	<b>50.7</b>

where  $\hat{y}_{te}$  denotes the pseudo labels of  $x_{te}$  obtained from the trained model in Eq. (8), and  $\mathcal{L}_{ce}$  is the cross-entropy loss as Eq. (1) describes.  $\text{Mix}(x^i, x^j) = \mathbf{M} \odot x^i + (1 - \mathbf{M}) \odot x^j$  denotes ClassMix operation, where  $\mathbf{M}$  is the class mask determined by the randomly selected class in image  $x^i$ .  $\mathcal{M}'_t$  offers the values of target model  $\mathcal{M}_t$  without gradient optimization.

Unlike the most closely related work [36] that reduces intra-domain gap by conducting intra-domain adversarial learning, our framework directly learns consistency representations for the target data in a semi-supervised learning manner. Notice that the adopted ClassMix technique can be considered to augment the target domain, which is more simple and stable than the adversarial learning method.

## 4 Experiments

### 4.1 Datasets

We demonstrate the efficacy of the proposed method on the standard adaptation tasks of GTA5 [6] $\rightarrow$ Cityscapes [22], SYNTHIA [7] $\rightarrow$ Cityscapes and Cityscapes $\rightarrow$ NTHU Cross-City [38]. The synthetic dataset GTA5 contains 24,966 annotated images with a resolution of  $1914 \times 1052$ , token from the famous game Grand Theft Auto. The ground truth is generated by the game render itself. SYNTHIA is another synthetic dataset, which contains 9,400 fully annotated images with the resolution of  $1280 \times 760$ . Cityscapes consists 2,975 annotated training images, and 500 validation images with the resolution of  $2048 \times 1024$ . NTHU Cross-City dataset has been recorded in four cities: Rome, Rio, Tokyo, and Taipei. Each city set has 3,200 unlabeled training images and 100 testing images with the resolution of  $2048 \times 1024$ . We employ the mean Intersection over Union (mIoU) as the evaluation metric which is widely adopted in semantic segmentation tasks.

### 4.2 Implementation Details

We use the DeepLab-V2 [39] architecture with ResNet-101 [40] pre-trained on ImageNet [41] as the backbone, which is the same as previous works [2–4]. We first pre-train the segmentation network on the source domain for 70k iterations to obtain a high-quality source model. Then it is considered as the initialization model. During training, we follow previous works [2–4] using Stochastic Gradient Descent (SGD) optimizer with the learning rate  $2.5 \times 10^{-4}$ , momentum 0.9, and weight decay  $5 \times 10^{-4}$ . We schedule the learning rate using ‘‘poly’’ policy: the learning rate is multiplied by  $(1 - \frac{iter}{max\_iter})^{0.9}$ . In the entropy minimization stage, we fix the classifier as mentioned above. In the other stages, the classifier is optimized with the learning rate  $2.5 \times 10^{-3}$ . Concerning the parameters, we utilize  $\alpha = 0.002$ ,  $\gamma = 3$ , and  $\lambda_{neg} = 0.05$  for all experiments. For self-training process, we assign the category-level top  $K = 65\%$  target predictions as pseudo-labels. We update pseudo labels epoch by epoch, and the maximum number of epochs is empirically set as 10. For the semi-supervised training process, we assign the target images with average entropy ranked top 30% as the easy group, and the other images are defined as the hard group. Generally, we randomly run our methods three times with different random seeds via **PyTorch** and report the average accuracy.

Table 2: Results of SYNTHIA  $\rightarrow$  Cityscapes. ‘‘SF’’ denotes the source data-free setting. **Red** is the best result for source data-free methods. **blue** is the best result for source data-dependent methods.

Method	SF	road	side.	build.	light	sign	vege.	sky	person	rider	car	bus	motor.	bike	mIoU
Source Only	-	45.2	19.6	71.9	5.5	7.8	75.3	81.9	57.3	17.3	39.0	19.5	7.0	25.7	36.4
AdaptSeg [2]	✗	79.2	37.2	78.8	9.9	10.5	78.2	80.5	53.5	19.6	67.0	29.5	21.6	31.3	45.9
ADVENT [4]	✗	<b>85.6</b>	42.2	79.7	5.4	8.1	80.4	<b>84.1</b>	57.9	23.8	73.3	36.4	14.2	33.0	48.0
CAG_UDA [42]	✗	84.8	41.7	<b>85.5</b>	13.7	23.0	<b>86.5</b>	78.1	<b>66.3</b>	28.1	81.8	21.8	22.9	49.0	<b>52.6</b>
SIM [44]	✗	83.0	<b>44.0</b>	80.3	17.1	15.8	80.5	81.8	59.9	<b>33.1</b>	70.2	37.3	28.5	45.8	52.1
FDA [5]	✗	79.3	35.0	73.2	<b>19.9</b>	<b>24.0</b>	61.7	82.6	61.4	31.1	<b>83.9</b>	<b>40.8</b>	<b>38.4</b>	<b>51.1</b>	52.5
SFDA [20]	✓	81.9	<b>44.9</b>	<b>81.7</b>	3.3	10.7	86.3	<b>89.4</b>	37.9	13.4	80.6	25.6	9.6	31.3	45.9
Sivaparased [19]	✓	59.3	24.6	77.0	<b>18.3</b>	<b>32.0</b>	<b>83.1</b>	80.4	46.3	17.8	76.7	17.0	18.5	34.6	45.0
DAS <sup>3</sup> (a)	✓	76.1	34.9	73.3	1.6	7.7	77.7	78.6	51.6	24.5	73.1	16.6	10.9	31.3	42.9
DAS <sup>3</sup> (b)	✓	80.8	38.0	76.4	0.0	9.3	80.7	84.5	55.9	30.3	75.6	35.4	<b>18.6</b>	53.2	49.1
DAS <sup>3</sup> (c)	✓	<b>82.9</b>	39.8	78.5	0.0	10.7	81.8	86.2	<b>62.1</b>	<b>35.4</b>	<b>81.3</b>	<b>44.1</b>	17.1	<b>56.8</b>	<b>52.1</b>

Table 3: Results of *black-box* source model on GTA5  $\rightarrow$  Cityscapes. ‘‘SF’’ denotes the source data-free setting.

Method	SF	road	side.	build.	wall	fence	pole	light	sign	vege.	terr.	sky	person	rider	car	truck	bus	train	motor.	bike	mIoU
Source only	-	75.8	16.8	77.2	12.5	21.0	25.5	30.1	20.1	81.3	24.6	70.3	53.8	26.4	49.9	17.2	25.9	6.5	25.3	36.0	36.5
DAS <sup>3</sup> + (b)	✓	74.8	23.6	78.9	27.4	17.5	24.1	34.0	24.9	82.6	25.7	74.3	58.6	31.7	71.5	31.4	6.9	0.0	34.8	45.4	40.4
DAS <sup>3</sup> + (c)	✓	83.3	24.2	80.3	29.7	22.4	26.3	33.0	25.5	84.7	35.7	76.6	61.9	34.0	81.7	32.1	17.3	0.0	42.1	53.4	44.4
DAS <sup>3</sup> + (aug)	✓	83.6	25.8	81.9	30.2	25.2	27.9	36.2	28.7	84.8	34.4	77.5	62.2	35.7	81.5	32.3	16.8	0.0	41.7	53.5	45.3

### 4.3 Results

We show the performance of our DAS<sup>3</sup> on GTA5 $\rightarrow$ Cityscapes in Table 1, SYNTHIA $\rightarrow$ Cityscapes in Table 2, and Cityscapes $\rightarrow$ Cross-City in Table 4. Model (a), (b), and (c) denote the different training stages described in Section 3. In addition, we compare our method with previous state-of-the-art works, including source data-dependent methods [2, 4, 23, 42–44, 5] and source data-free methods [20, 19]. The utility of source data can directly align distributions of source and target domains by adversarial learning [2, 4]. Thus they obtain higher performance reasonably. Notice that our method without source data performs comparable to or even better than the methods with source data. Furthermore, concerning source data-free methods, our method outperforms previous works [20, 19] with a large margin.

Specifically, for the tasks of GTA5 $\rightarrow$ Cityscapes and SYNTHIA $\rightarrow$ Cityscapes, shown in Table 1 and 2, our method arrives at the mIoU score 50.7% and 52.1%, respectively, which offers performance gain by 14.2% and 15.7% compared with the non-adaptation baseline (Source Only). Moreover, the proposed method surpasses two existing source data-free methods [20] and [19] by 5.4% and 7.1% mIoU score, respectively. Compared with the adaptation methods using source data, our method even outperforms or achieves competitive results to them. These results verify the effectiveness of our method.

Table 4 shows the results on Cityscapes $\rightarrow$ Cross-City task. For clear description, we only report the mIoU scores in four different cities. The results demonstrate the effectiveness of our method for minor domain shift adaptation, achieving the best results in Rome, Rio, Tokyo, and Taipei.

### 4.4 Performance for Black-box Source Model

We also conduct experiments for black-box source model [45], where only the source model’s predictions are available. Due to no access of trained source model, the implicit feature alignment is impractical. Consequently, we apply our bi-directional self-training strategy and information propagation to tackle black-box source model scenario. This situation is more challenging and interesting in practice, because it does not require any source model details but the network outputs.

We report GTA5→Cityscapes results in Table 3. “DAS<sup>3</sup>+ (b)” and “DAS<sup>3</sup>+ (c)” represent our black-box source model on bi-directional self-training stage and information propagation stage, respectively. “DAS<sup>3</sup>+ (aug)” denotes our black-box source model results using data augmentation techniques. From the results, we can observe that our method is suitable for black-box source model situation with the performance of 45.3%, comparing to the source only model 36.5% mIoU.

Table 4: Results of Cityscapes → Cross-City. Table 5: Ablation study of each proposed component on GTA5→Cityscapes task.

Method	SF	Rome	Rio	Tokyo	Taipei
Source Only	-	46.4	45.1	44.1	44.1
ADVENT [4]	✗	47.3	46.8	45.5	45.1
AdaptSegNet [2]	✗	48.0	47.8	46.2	45.1
Cros-City [38]	✗	42.9	42.5	42.8	39.6
MaxSquare [9]	✗	<b>48.5</b>	<b>48.7</b>	<b>47.1</b>	<b>47.2</b>
SFDA [20]	✓	48.3	49.0	46.4	47.2
Sivaparased [19]	✓	53.8	53.5	49.8	50.1
DAS <sup>3</sup> (a)	✓	48.2	48.7	45.3	43.6
DAS <sup>3</sup> (b)	✓	53.8	55.3	48.6	47.8
DAS <sup>3</sup> (c)	✓	<b>55.9</b>	<b>57.8</b>	<b>50.5</b>	<b>51.1</b>

Model	$\mathcal{L}_{fel}$	$\mathcal{L}_{div}$	$\mathcal{L}_{ppl}$	$\mathcal{L}_{npl}$	$\mathcal{L}_{mix}$	Aug.	mIoU	gain ( $\Delta$ )
Source							36.5	-
(a)	✓						41.7	+5.2
(b)	✓	✓					42.1	+0.4
(c)	✓	✓	✓				45.3	+3.2
(d)	✓	✓	✓	✓			46.7	+1.4
(e)	✓	✓	✓	✓	✓		50.7	+4.0
(f)	✓	✓	✓	✓	✓	✓	<b>51.1</b>	+0.4

#### 4.5 Ablation Study

Table 5 reveals the improvement of proposed components compared to the “source-only” baseline on GTA5→Cityscapes adaptation task, by progressively adding each module into the system. As Table 5 shows, we can observe that each component contributes to adaptation, with achieving the final performance of 51.1%, outperforming the “source-only” baseline by 14.6%.

**Influence of implicit feature alignment.** From the model (a) and (b) in Table 5, we can observe that our focal entropic loss and weighted diversity loss can provide a significant margin improvement for adaptation. Specifically, model (a) with focal entropic loss achieves a 41.6% mIoU result, which surpasses source only model by 5.2 points. It also outperforms the previous entropy minimization method [19] reported mIoU result as 19.8%. Furthermore, model (b) with additional weighted diversity loss boosts the performance improvement with 0.4 mIoU, revealing that diversity enforcing is important for our setting.

**Influence of bi-directional self-training.** For the bi-directional self-training process, we ablate the positive pseudo labeling and negative pseudo labeling, respectively. From the results, we observe that model (c) trained from positive pseudo labeling provides 3.2 point gains compared to model (b). It is reasonable that the positive pseudo labels enhance feature representations for target data. On the other hand, our negative pseudo labeling (model (d)) fancily offers 1.4 point improvement based on the model (c). This result demonstrates that the proposed negative pseudo labeling indeed helps to learn decision boundaries and is complementary to traditional positive labeling methods.

**Influence of information propagation.** To testify the effectiveness of the proposed information propagation strategy, we report the result of model (e) in Table 5, which provides a significant improvement with 4.0 mIoU compared to the model (d). It demonstrates our semi-supervised technique is simple and effective for reducing intra-domain discrepancy. Furthermore, we adopt data augmentation strategies (*e.g.*, color jitter, Gaussian Blur) to enhance the robustness, achieving the performance of 51.1% as shown in model (f).

#### 4.6 Parameter Sensitivity Analysis

Our framework contains two new hyper-parameters  $\alpha$  and  $\gamma$  in Eq. (2). To analyze the influence of them, we conduct experiments on the GTA5→Cityscapes task. We select the value of  $\alpha$  from the range of [0.001, 0.002, 0.003],  $\gamma$  from the range of [0, 1, 2, 3, 4, 5], respectively. The results are shown in Figure 3(a). Although our experiments set  $\alpha = 0.002$  and  $\gamma = 3$  since it peaks, we observe that the focal entropic loss is relatively robust to these parameters. Furthermore, we also optimize the model without freezing the source classifier. The performance drops significantly compared to our

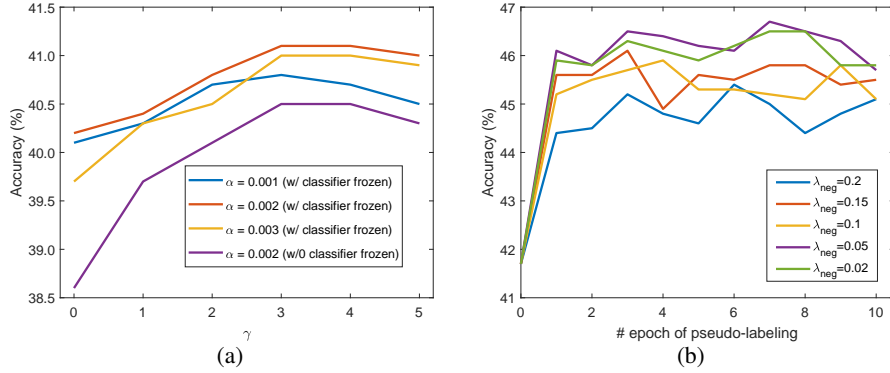


Figure 3: (a) Analysis for the hyper-parameters  $\alpha$  and  $\gamma$  of the proposed focal entropic loss. (b) Robustness to the negative threshold  $\lambda_{neg}$  for the proposed negative pseudo assignment method.

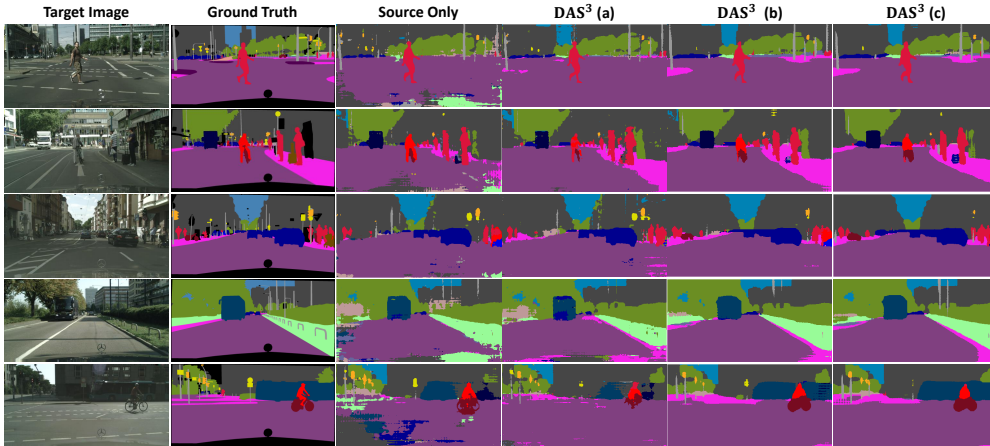


Figure 4: Visualization for predicted segmentation masks on the GTA5→Cityscapes task.

method with the classifier frozen, which indicates that the implicit alignment with source classifier frozen is essential.

Figure 3(b) shows the test accuracy when varying the assignment threshold  $\lambda_{neg}$  related to negative pseudo labels in Eq. (6). It shows that the proposed negative pseudo labeling method is relatively robust to this hyper-parameter. Moreover, the proposed method quickly converges after several training epochs. We also observe that  $\lambda_{neg} < 0.1$  obtains a satisfactory performance compared to those when  $\lambda_{neg} > 0.1$ . This may be because that more noise labels are introduced when the threshold increases because our negative pseudo labeling method focuses on the predictions with lower confidence scores.

#### 4.7 Visualization

We visualize the masks predicted by our method and compare the results to those predicted by the “Source-Only” network in Figure 4. To show the contribution of each stage, we add each component progressively and provide qualitative results of “DAS<sup>3</sup> (a)”, “DAS<sup>3</sup> (b)”, and “DAS<sup>3</sup> (c)”, respectively. It is evident that even without source data, our method achieves reliable results with fewer spurious areas. Furthermore, compared to the “Source Only” model, each stage contributes a lot in terms of pixel-level accuracy.

## 5 Conclusion

This paper presents a novel source data-free framework for domain adaptive semantic segmentation called DAS<sup>3</sup>. In the absence of source data, DAS<sup>3</sup> focuses on transferring knowledge from the source model via implicit feature alignment and subsequently exploit target-specific knowledge to reduce the intra-domain discrepancy. We conduct extensive experiments and ablation studies to validate the effectiveness of the proposed framework. Extensive experiments and ablation studies are conducted to validate the effectiveness of the proposed DAS<sup>3</sup>. On the standard adaptation tasks, DAS<sup>3</sup> achieves new state-of-the-art results and performs comparable to source data-dependent adaptation methods.

## References

- [1] Long, J., E. Shelhamer, T. Darrell. Fully convolutional networks for semantic segmentation. In *Proc. CVPR*, pages 3431–3440. 2015.
- [2] Tsai, Y.-H., W.-C. Hung, S. Schulter, et al. Learning to adapt structured output space for semantic segmentation. In *Proc. CVPR*, pages 7472–7481. 2018.
- [3] Luo, Y., L. Zheng, T. Guan, et al. Taking a closer look at domain shift: Category-level adversaries for semantics consistent domain adaptation. In *Proc. CVPR*, pages 2507–2516. 2019.
- [4] Vu, T.-H., H. Jain, M. Bucher, et al. Advent: Adversarial entropy minimization for domain adaptation in semantic segmentation. In *Proc. CVPR*, pages 2517–2526. 2019.
- [5] Yang, Y., S. Soatto. Fda: Fourier domain adaptation for semantic segmentation. In *Proc. CVPR*, pages 4085–4095. 2020.
- [6] Richter, S. R., V. Vineet, S. Roth, et al. Playing for data: Ground truth from computer games. In *Proc. ECCV*, pages 102–118. 2016.
- [7] Ros, G., L. Sellart, J. Materzynska, et al. The synthia dataset: A large collection of synthetic images for semantic segmentation of urban scenes. In *Proc. CVPR*, pages 3234–3243. 2016.
- [8] Hong, W., Z. Wang, M. Yang, et al. Conditional generative adversarial network for structured domain adaptation. In *Proc. CVPR*, pages 1335–1344. 2018.
- [9] Chen, M., H. Xue, D. Cai. Domain adaptation for semantic segmentation with maximum squares loss. In *Proc. ICCV*, pages 2090–2099. 2019.
- [10] Hoffman, J., E. Tzeng, T. Park, et al. CyCADA: Cycle-consistent adversarial domain adaptation. In *Proc. ICML*, pages 1989–1998. 2018.
- [11] Liang, J., R. He, Z. Sun, et al. Distant supervised centroid shift: A simple and efficient approach to visual domain adaptation. In *Proc. CVPR*, pages 2975–2984. 2019.
- [12] Chen, Y.-C., Y.-Y. Lin, M.-H. Yang, et al. Crdoco: Pixel-level domain transfer with cross-domain consistency. In *Proc. CVPR*, pages 1791–1800. 2019.
- [13] Choi, J., T. Kim, C. Kim. Self-ensembling with gan-based data augmentation for domain adaptation in semantic segmentation. In *Proc. ICCV*, pages 6830–6840. 2019.
- [14] Sankaranarayanan, S., Y. Balaji, A. Jain, et al. Learning from synthetic data: Addressing domain shift for semantic segmentation. In *Proc. CVPR*, pages 3752–3761. 2018.
- [15] Wu, Z., X. Wang, J. E. Gonzalez, et al. Ace: Adapting to changing environments for semantic segmentation. In *Proc. ICCV*, pages 2121–2130. 2019.
- [16] Kim, M., H. Byun. Learning texture invariant representation for domain adaptation of semantic segmentation. In *Proc. CVPR*, pages 12975–12984. 2020.
- [17] Chang, W.-L., H.-P. Wang, W.-H. Peng, et al. All about structure: Adapting structural information across domains for boosting semantic segmentation. In *Proc. CVPR*, pages 1900–1909. 2019.
- [18] Tsai, Y.-H., K. Sohn, S. Schulter, et al. Domain adaptation for structured output via discriminative patch representations. In *Proc. ICCV*, pages 1456–1465. 2019.
- [19] S, P. T., F. Fleuret. Uncertainty reduction for model adaptation in semantic segmentation. In *Proc. CVPR*, pages 9613–9623. 2021.

- [20] Liu, Y., W. Zhang, J. Wang. Source-free domain adaptation for semantic segmentation. In *Proc. CVPR*, pages 1215–1224. 2021.
- [21] Olsson, V., W. Tranheden, J. Pinto, et al. Classmix: Segmentation-based data augmentation for semi-supervised learning. In *Proc. WACV*, pages 1369–1378. 2021.
- [22] Cordts, M., M. Omran, S. Ramos, et al. The cityscapes dataset for semantic urban scene understanding. In *Proc. CVPR*, pages 3213–3223. 2016.
- [23] Zou, Y., Z. Yu, B. Vijaya Kumar, et al. Unsupervised domain adaptation for semantic segmentation via class-balanced self-training. In *Proc. ECCV*, pages 289–305. 2018.
- [24] Zou, Y., Z. Yu, X. Liu, et al. Confidence regularized self-training. In *Proc. ICCV*, pages 5982–5991. 2019.
- [25] Zheng, Z., Y. Yang. Rectifying pseudo label learning via uncertainty estimation for domain adaptive semantic segmentation. *International Journal of Computer Vision*, 129(4):1106–1120, 2021.
- [26] Lian, Q., F. Lv, L. Duan, et al. Constructing self-motivated pyramid curriculums for cross-domain semantic segmentation: A non-adversarial approach. In *Proc. ICCV*, pages 6758–6767. 2019.
- [27] Subhani, M. N., M. Ali. Learning from scale-invariant examples for domain adaptation in semantic segmentation. In *Proc. ECCV*, pages 290–306. 2020.
- [28] Liang, J., D. Hu, J. Feng. Do we really need to access the source data? source hypothesis transfer for unsupervised domain adaptation. In *Proc. ICML*, pages 6028–6039. 2020.
- [29] Chidlovskii, B., S. Clinchant, G. Csurka. Domain adaptation in the absence of source domain data. In *Proc. KDD*, pages 451–460. 2016.
- [30] Li, R., Q. Jiao, W. Cao, et al. Model adaptation: Unsupervised domain adaptation without source data. In *Proc. CVPR*, pages 9641–9650. 2020.
- [31] Kundu, J. N., N. Venkat, R. V. Babu, et al. Universal source-free domain adaptation. In *Proc. CVPR*, pages 4544–4553. 2020.
- [32] Miyato, T., S.-i. Maeda, M. Koyama, et al. Virtual adversarial training: a regularization method for supervised and semi-supervised learning. *IEEE Transactions on Pattern Analysis and Machine Intelligence*, 41(8):1979–1993, 2018.
- [33] Verma, V., A. Lamb, J. Kannala, et al. Interpolation consistency training for semi-supervised learning. In *Proc. IJCAI*, pages 3635–3641. 2019.
- [34] Xie, Q., Z. Dai, E. Hovy, et al. Unsupervised data augmentation for consistency training. In *Proc. NeurIPS*, pages 6256–6268. 2020.
- [35] Berthelot, D., N. Carlini, E. D. Cubuk, et al. Remixmatch: Semi-supervised learning with distribution alignment and augmentation anchoring. In *Proc. ICLR*. 2019.
- [36] Pan, F., I. Shin, F. Rameau, et al. Unsupervised intra-domain adaptation for semantic segmentation through self-supervision. In *Proc. ICCV*, pages 3764–3773. 2020.
- [37] Lin, T.-Y., P. Goyal, R. Girshick, et al. Focal loss for dense object detection. In *Proc. ICCV*, pages 2980–2988. 2017.
- [38] Chen, Y.-H., W.-Y. Chen, Y.-T. Chen, et al. No more discrimination: Cross city adaptation of road scene segmenters. In *Proc. ICCV*, pages 1992–2001. 2017.
- [39] Chen, L.-C., G. Papandreou, I. Kokkinos, et al. Deeplab: Semantic image segmentation with deep convolutional nets, atrous convolution, and fully connected crfs. *IEEE Transactions on Pattern Analysis and Machine Intelligence*, 40(4):834–848, 2017.
- [40] He, K., X. Zhang, S. Ren, et al. Deep residual learning for image recognition. In *Proc. CVPR*, pages 770–778. 2016.
- [41] Deng, J., W. Dong, R. Socher, et al. Imagenet: A large-scale hierarchical image database. In *Proc. CVPR*, pages 248–255. 2009.
- [42] Zhang, Q., J. Zhang, W. Liu, et al. Category anchor-guided unsupervised domain adaptation for semantic segmentation. In *Proc. NeurIPS*, pages 433–443. 2019.

- [43] Kang, G., Y. Wei, Y. Yang, et al. Pixel-level cycle association: A new perspective for domain adaptive semantic segmentation. In *Proc. NeurIPS*, pages 3569–3580. 2020.
- [44] Wang, Z., M. Yu, Y. Wei, et al. Differential treatment for stuff and things: A simple unsupervised domain adaptation method for semantic segmentation. In *Proc. CVPR*, pages 12635–12644. 2020.
- [45] Liang, J., D. Hu, R. He, et al. Distill and fine-tune: Effective adaptation from a black-box source model. *arXiv:2104.01539*, 2021.